Journal of Sound and Vibration (1997) **205**(5), 631–645

COMPUTING STATICALLY COMPLETE FLEXIBILITY FROM DYNAMICALLY MEASURED FLEXIBILITY

S. W. DOEBLING

Engineering Sciences and Applications Division, Engineering Analysis Group (ESA-EA), Los Alamos National Laboratory, M/S P946, Los Alamos, NM, 87545, U.S.A.

AND

L. D. PETERSON

Center for Aerospace Structures and Department of Aerospace Engineering Sciences, University of Colorado, Boulder, CO 80309-0429, U.S.A.

(*Received* 10 *May* 1996; *and in final form* 21 *March* 1997)

A method is presented for computing a statically complete structural flexibility matrix from a dynamically measured flexibility matrix. When computed from a limited set of measured modal data, dynamically measured flexibility cannot reproduce the correct static force–displacement relations of the structure, i.e., it is not "statically complete." A previously developed algorithm is used to include the effects of residual flexibility in the dynamically measured flexibility matrix, so that certain entries in the measured flexibility matrix can be considered to be statically complete. The method presented in this paper computes the remainder of the entries in the statically complete flexibility matrix by first forming a static flexibility matrix using assumed stiffness parameters and elemental connectivity, then scaling it such that it approximates the corresponding statically complete entries in the measured flexibility matrix. The method requires the solution of linear systems of equations only. The method is derived and applied to both numerical and experimental measured flexibility matrices, and the improved accuracy of the static flexibility over the dynamically measured flexibility is demonstrated.

1. INTRODUCTION

The static flexibility matrix has become a widely used tool for the analysis of structures. It has been used for structural damage assessment [1–5], component-mode model synthesis [6, 7], and for the analysis of non-linear mechanisms [8]. The flexibility matrix can be approximated from measured mode shapes and modal frequencies, or it can be measured directly using static load-deflection testing. However, it should be noted that static testing has some disadvantages compared to vibration testing, such as instrumentation and boundary condition issues. The more common technique is the synthesis of an approximate flexibility matrix from measured modal data. Because of the standard methods and equipment available for extraction of the modal data, the synthesis of the flexibility matrix using the measured modes and frequencies is straighforward.

The primary disadvantage of using the measured flexibility matrix as synthesized from the measured modal parameters is the issue of static completeness. Because a structure contains an infinite number of modes, and all of these modes are required to fully define the static load-displacement relationship between the instrumented degrees of freedom

0022–460X/97/350631 + 15 $25.00/0/sv971050

(DOF), the measured flexibility matrix is generally not "statically complete." In this context, statically complete refers to the ability of the stiffness or flexibiliy matrix to reproduce the correct static load-displacement relationship between the corresponding DOF.

One way to produce a statically complete flexibility matrix from dynamically measured modal parameters is by including the effects of the residual flexibility matrix. The residual flexibility matrix represents the contributions of the unmeasured modes to the statically complete flexibility matrix. Unfortunately, only one column of the residual flexibility matrix is obtained for each measurement DOF which has a modal excitation applied to it. Providing a modal excitation at each DOF would result in a statically complete, dynamically measured flexibility matrix, but is most often impractical due to issues of testing time, accessibility of the DOF, etc. In many data sets, the magnitude of the residual flexibility compared to the magnitude of the flexibility of the measured modes is small enough so that the dynamically measured flexibility is considered to be statically complete to a certain degree of precision. However, this level of precision is often not sufficient, and so the dynamically measured flexibility matrix is generally not statically complete except at those few entries where the residual flexibility is known.

In this paper, a technique is proposed for synthesizing a statically complete flexibility matrix which reproduces specific partitions of the dynamically measured flexibility matrix. A statically complete flexibility matrix based on the assumed elemental connectivity of the structure is scaled such that it reproduces (approximately) the statically complete partitions of the dynamically measured flexibility matrix (i.e., those partitions where the residual flexibility is known). The appropriate partitions of this scaled flexibility matrix are then combined with the statically complete partitions of the dynamically measured flexibility matrix to produce a nearly statically complete flexibility matrix.

The remainder of the paper is organized as follows: first, the theory behind the algorithm is presented, including an overview of the dynamically measured flexibility matrix, the parameterization of the statically complete flexibility matrix, and the scaling procedure. Second, the method is applied to numerical simulations of a cantilevered beam. Next, the method is demonstrated on experimental data from a cantilevered beam. Finally, a summary of the findings and conclusions are presented.

2. THE DYNAMICALLY MEASURED FLEXIBILITY MATRIX

The matrix of static flexibility influence coefficients, or *static flexibility matrix*, $[G]$, is the inverse of the structural stiffness matrix, such that

$$\{\mathbf{u}\} = [\mathbf{G}]\{\mathbf{F}\}, \tag{1}$$

where $\{\mathbf{F}\}$ is the vector of applied static loads, and $\{\mathbf{u}\}$ is the vector of resulting static responses The physical interpretation of the static flexibility matrix can be seen by inspection of equation (1). Suppose that a unit force is applied at a certain DOF, such that the static force vector $\{\mathbf{F}\}$ has a value of unity at one DOF and zero at all other DOF. By equation (1), the resulting static deflections $\{\mathbf{u}\}$ will be equal to the column of $[\mathbf{G}]$ corresponding to the DOF where the force was applied. Thus, for a restrained structure, the columns of $[\mathbf{G}]$ represent the static deformations resulting from the application of a unit force at each successive DOF. For an unrestrained structure, they represent the inertia-relief deformation shapes resulting from such a load.

The static flexibility matrix can be computed using the measured vibration modes and the residual flexibility as

$$[\mathbf{G}] = [\mathbf{\Phi}_{\mathrm{n}}][\mathbf{\Lambda}_n]^{-1}[\mathbf{\Phi}_n]^{\mathrm{T}} + [\mathbf{G}_r], \tag{2}$$

where $[\mathbf{\Phi}_n]$ is the matrix of mass-normalized structural eigenvectors (measured vibration mode shapes) at a given set of measurement DOF, $[\mathbf{\Lambda}_n]$ is the diagonal matrix of structural eigenvalues (the squares of the measured circular modal frequencies) and $[\mathbf{G}_r]$ is the residual flexibility (the contribution of the unmeasured vibration modes). Thus the static flexibility matrix $[\mathbf{G}]$ can be reconstructed from the measured dynamic properties of the system. This representation is statically complete, meaning that the full static response of the structure can be reproduced between any of the DOF in the measurement set.

The primary drawback to computing the flexibility matrix using measured vibration modes is that only particular partitions of the residual flexibility matrix can be measured. Specifically, only one column (and corresponding row, because of symmetry) of the residual flexibility matrix can be obtained for each DOF where modal excitation is provided. Thus, under practical testing constraints, the dynamically measured flexibility matrix is generally not statically complete.

A method for estimating a rank-deficient solution for the full-DOF residual flexibility matrix is derived in reference [9]. This derivation starts by partitioning the residual flexibility matrix at the measurement DOF with respect to the driving point DOF, $\{\mathbf{q}_d\}$, and the non-driving point measurement DOF, $\{\mathbf{q}_s\}$. Partitioning the full residual flexibility matrix according to these definitions yields

$$[\mathbf{G}_r] = \begin{bmatrix} \mathbf{G}_{r_{dd}} & \mathbf{G}_{r_{sd}}^{\mathrm{T}} \\ \mathbf{G}_{r_{sd}} & \mathbf{G}_{r_{ss}} \end{bmatrix}, \tag{3}$$

where the subscript r denotes residual flexibility and the subscripts s and d correspond to DOF sets $\{\mathbf{q}_s\}$ and $\{\mathbf{q}_d\}$, respectively. It is shown in reference [9] that the partitions of the residual flexibility matrix that can be identified from the measured frequency response data are

$$[\mathbf{G}_{r_d}] = \begin{bmatrix} \mathbf{G}_{r_{dd}} \\ \mathbf{G}_{r_{sd}} \end{bmatrix} \tag{4}$$

because these are the partitions which correspond to the DOF in the measured frequency response function matrix. This is apparent when one notes that the frequency response function matrix contains an entry at each frequency line for each sensor measurement (the union of sets $\{\mathbf{q}_s\}$ and $\{\mathbf{q}_d\}$) with respect to the driving point set $\{\mathbf{q}_d\}$. Therefore, the partitions in equation (4), $[\mathbf{G}_{r_{dd}}]$ and $[\mathbf{G}_{r_{sd}}]$, can be estimated directly from the measured data, so that the entries of the residual flexibility matrix which lie along the rows and columns corresponding to the driving point DOF are known.

A solution for the unmeasured partition of the residual flexibility matrix, $[\mathbf{G}_{r_{ss}}]$, which preserves modal orthogonality, has a lower bound of

$$[\mathbf{G}_{r_{ss}}^{o}] = [\mathbf{G}_{r_{sd}}][\mathbf{G}_{r_{dd}}]^{-1}[\mathbf{G}_{r_{sd}}]^{\mathrm{T}}, \tag{5}$$

as shown in reference [9]. This solution does not add any rank (i.e., no independent information) to the residual flexibility matrix, but does allow the estimation of the rank-deficient dynamically measured flexibility matrix

$$[\mathbf{G}^o] = [\mathbf{\Phi}_n][\mathbf{\Lambda}_n]^{-1}[\mathbf{\Phi}_n]^{\mathrm{T}} + \begin{bmatrix} \mathbf{G}_{r_{dd}} & \mathbf{G}_{r_{sd}}^{\mathrm{T}} \\ \mathbf{G}_{r_{sd}} & \mathbf{G}_{r_{ss}}^{o} \end{bmatrix}. \tag{6}$$

The solution presented in equation (6) is not statically complete, but can be computed using only measured data. The entries in the dynamically measured flexibility matrix which lie along the rows or columns corresponding to the driving point DOF can be considered to be statically complete, because the corresponding entries in the residual flexibility matrix are measured. The entries in $[\mathbf{G}^o]$ corresponding to the driving point DOF can thus be used as a baseline for the scaling of the corresponding entries in the statically complete flexibility matrix, as described in the next section.

3. COMPUTATION OF THE STATICALLY COMPLETE FLEXIBILITY MATRIX

The procedure for computing a statically complete flexibility matrix, $[\mathbf{G}^c]$, from dynamically measured flexibility is diagrammed in Figure 1 and presented in this section. A brief synopsis of the method is as follows: first, the dynamically measured flexibility matrix $[\mathbf{G}^o]$ is computed, including the residual flexibility terms, as shown in equation (6). This matrix contains certain entries which are considered to be accurate (those associated with the driving point DOF), and others which are known to be inaccurate (those approximated using equation (5)). The idea of the method is to use the entries in $[\mathbf{G}^o]$ which are known to a high level of accuracy in conjunction with an assumed finite element model (FEM) structural connectivity to improve the accuracy of the remaining entries in $[\mathbf{G}^o]$ (i.e., those computed using equation (5)). The use of an assumed FEM structural connectivity model ensures that the resulting flexibility matrix $[\mathbf{G}^c]$ will be statically complete.

The procedure begins with the determination of the dynamically measured flexibility, including the effects of residual flexibility (as described in the previous section). That step is labeled as Step 1 in Figure 1. The resulting flexibility matrix, $[\mathbf{G}^o]$, has certain entries which are directly computed from the data and certain entries that are estimated using the approximation of equation (5).

The next step is the parameterization of the statically complete flexibility matrix (Step 2). This step determines the form of all possible statically complete flexibility matrices which have the assumed FEM structural connectivity, and also ensures that the resulting flexibility matrix will be statically complete. This step begins with the determination of a global stiffness matrix $[\mathbf{K}]$ from a finite element model, which can be as simple or complex as desired. The stiffness matrix $[\mathbf{K}]$ is statically complete by definition, and therefore so is the corresponding flexibility matrix

$$[\mathbf{G}] \equiv [\mathbf{K}]^{+}, \tag{7}$$

where the operator $+$ represents the *Moore–Penrose pseudoinverse* [10]. This relation implies that the flexibility matrix is uniquely determined by the same underlying connectivity and elemental stiffness matrices as the global stiffness matrix. (It should be noted that a statically complete flexibility matrix may be rank-deficient if the structure contains rigid body modes. The use of the pseudoinverse rather than a strict inverse in equation (7) ensures that the transformation will be valid in this case). The

parameterization can be written as the singular value decomposition of the flexibility matrix.

$$[\mathbf{G}] = [\mathbf{V}][\mathbf{\Sigma}][\mathbf{V}]^{\mathrm{T}}, \tag{8}$$

where diag($[\mathbf{\Sigma}]$) are the singular values of $[\mathbf{G}]$, and $[\mathbf{V}]$ are the singular vectors of $[\mathbf{G}]$. Thus, $[\mathbf{V}]$ determines the co-ordinate basis for the statically complete flexibility matrix and $[\mathbf{\Sigma}]$ determines the scaling.

After Step 2 is completed, a statically complete flexibility matrix exists, as defined in equation (7), but it does not necessarily agree with the measured flexibility matrix $[\mathbf{G}^o]$ because it was generated using assumed values for the finite element model parameters.

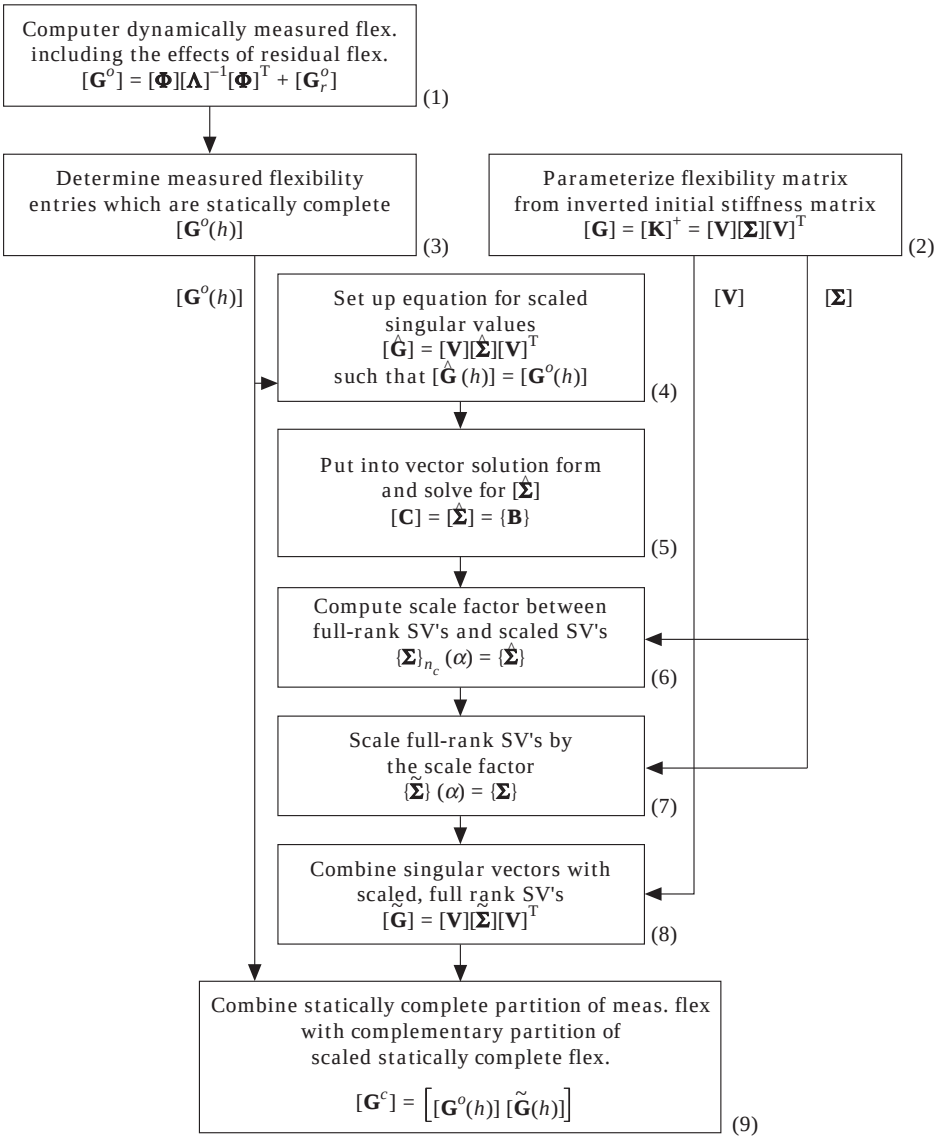

Figure 1. Flowchart of the statically complete flexibility estimation procedure (numbers in parenthesis indicate solution steps).

The remainder of the method is a procedure to scale this statically complete flexibility matrix to match those entries in $[\mathbf{G}^o]$ which are assumed to be most accurate. The result will be a statically complete flexibility matrix which agrees to a high level of accuracy with the measured data.

The next step (Step 3) is the selection of which statically complete entries in the dynamically measured flexibility matrix will be used to scale the parameterized flexibility matrix. These entries are the entries in $[\mathbf{G}^0]$ which are assumed to be the most accurate. Typically, these entries are chosen such that they correspond to the driving point degrees of freedom, because those DOF typically have the most accurate values for residual flexibility. Those entries which are assumed to be the most accurate are defined as the "correlation set" of DOF for the scaling process. The set of DOF which has directly measurable residual flexibility consists of the measurement sensor DOF $\{\mathbf{q}_s\}$ plus the excitation DOF set $\{\mathbf{q}_d\}$. Application to experimental data has shown that some DOF should be left out of the correlation set because even though the residual flexibility is directly measurable the accuracy may be poor. For example, rotational DOF which are resolved from translational measurements or DOF where the response has extremely low magnitude (and therefore high sensitivity to noise) should be excluded from the measurement set. These guidelines are used to select which DOF have the most accurate residual flexibility measurements, which allows the definition of the correlation set $[\mathbf{h}]$ as

$$[\mathbf{h}] = \begin{bmatrix} i_1 & j_1 \\ i_2 & j_2 \\ \vdots & \vdots \\ i_{n_h} & j_{n_h} \end{bmatrix}, \tag{9}$$

where i and j are the row and column co-ordinates of the entries in $[\mathbf{G}^o]$ to be correlated. Because the correlation set is the set of n_h flexibility coefficients in $[\mathbf{G}^o]$ which are considered to be the most accurate, these entries will be used to scale the corresponding entries in $[\mathbf{G}]$. Note that because of symmetry, only the values in the upper or lower triangle of the flexibility matrix need to be correlated. We define the co-ordinates of the remaining entries to be the uncorrelated set $[\bar{\mathbf{h}}]$, which is the complementary set of $[\mathbf{h}]$.

Next, the parameterized flexibility matrix from equation (8) is scaled to match the entries of the dynamically measured flexibility matrix $[\mathbf{G}^o]$ defined as $[\mathbf{h}]$ in Step 3. This part of the method encompasses Steps 4–8. These steps are accomplished by scaling the singular values $[\mathbf{\Sigma}]$ of the parameterized flexibility matrix. The resulting scaled flexibility matrix is termed $[\tilde{\mathbf{G}}]$, and is statically complete by the definition of $[\mathbf{G}]$ in equation (7).

Step 4 begins by assuming a set of singular values $[\hat{\mathbf{\Sigma}}]$ can be computed such that the $[\mathbf{h}]$ entries in $[\mathbf{V}][\hat{\mathbf{\Sigma}}][\mathbf{V}]^{\mathrm{T}}$ are a least-squares fit to the $[\mathbf{h}]$ entries in $[\mathbf{G}^o]$. Mathematically, this step can be expressed as: compute $[\hat{\mathbf{\Sigma}}]$ such that

$$[\hat{\mathbf{G}}(h)] = [\mathbf{G}^o(h)], \tag{10}$$

where

$$[\hat{\mathbf{G}}] = [\mathbf{V}][\hat{\mathbf{\Sigma}}][\mathbf{V}]^{\mathrm{T}} \tag{11}$$

and where $[\mathbf{G}^o(h)]$ represents the $[\mathbf{h}]$ entries in $[\mathbf{G}^o]$, and $[\hat{\mathbf{G}}(h)]$ represents the $[\mathbf{h}]$ entries in $[\hat{\mathbf{G}}]$. Since $[\hat{\mathbf{\Sigma}}]$ is diagonal equation (10) can be solved (Step 5) by solving the system defined by

$$[\mathbf{C}]\{\hat{\mathbf{\Sigma}}\} = \{\mathbf{B}\}, \tag{12}$$

where $\{\mathbf{B}\}$ is the vector of the entries in $[\mathbf{G}^0(h)]$, and the rth row of $[\mathbf{C}]$ is defined as

$$[\mathbf{C}_r] = [(V(i_r, 1)V(j_r, 1)) \cdots (V(i_r, n_s)V(j_r, n_s))], \tag{13}$$

where n_s is the number of non-zero singular values in $\{\hat{\mathbf{\Sigma}}\}$. When n_h is smaller than the rank of $[\mathbf{G}]$, then $n_s = n_h$, otherwise, $n_s = \text{rank}([\mathbf{G}])$.

Since the number of entries in $[\mathbf{G}^o(h)]$, n_h, is generally smaller than the rank of $[\mathbf{G}]$, the n_s non-zero singular values in $\{\hat{\mathbf{\Sigma}}\}$ must be augmented so that the rank of $[\mathbf{G}]$ is preserved,

$$\text{rank}([\mathbf{G}]) = \text{rank}([\hat{\mathbf{G}}]). \tag{14}$$

Preserving the rank of $[\mathbf{G}]$ is critical to ensuring that the result will be statically complete. This augmentation must be done such that the magnitudes of the singular values $\{\hat{\mathbf{\Sigma}}\}$ are preserved, and such that the ratios of the singular values $\{\mathbf{\Sigma}\}$ of the statically complete flexibility matrix $[\mathbf{G}]$ are preserved. The most direct way to accomplish both of these goals is to select a number of singular values to scale, n_c, then scale $\{\mathbf{\Sigma}\}$ such that its n_c largest entries $\{\mathbf{\Sigma}\}_{n_c}$ match the entries $\{\hat{\mathbf{\Sigma}}\}$ as closely as possible. Because there are n_s singular values in $\{\hat{\mathbf{\Sigma}}\}$, then $n_c \leqslant n_s$. This scaling can be accomplished by solving for the scalar value α in a least-squares sense (Step 6) such that

$$\{\mathbf{\Sigma}\}_{n_c}(\alpha) = \{\hat{\mathbf{\Sigma}}\} \tag{15}$$

and then scaling all of $\{\mathbf{\Sigma}\}$ (Step 7) to get the full-rank set of scaled singular values $\{\tilde{\mathbf{\Sigma}}\}$,

$$\{\tilde{\mathbf{\Sigma}}\} = (\alpha)\{\mathbf{\Sigma}\}. \tag{16}$$

These scaled singular values can then be combined with the original statically complete flexibility singular vectors $[\mathbf{V}]$ (Step 8) to get

$$[\tilde{\mathbf{G}}] = [\mathbf{V}][\tilde{\mathbf{\Sigma}}][\mathbf{V}]^{\mathrm{T}}. \tag{17}$$

So the resulting matrix $[\tilde{\mathbf{G}}]$ is statically complete, but also accurately represents the $[\mathbf{h}]$ entries in $[\mathbf{G}^o]$.

Recall that the $[\mathbf{h}]$ entries in $[\mathbf{G}^o]$ are considered to be the most accurate values available for these entries. Thus, it is desirable to preserve these values exactly in the final solution. However, the $[\bar{\mathbf{h}}]$ entries in $[\tilde{\mathbf{G}}]$ are considered to be the most accurate values available for those entries, so it is also desirable to preserve those values exactly in the final solution. Therefore, the final step (Step 9) is the combination of the $[\mathbf{h}]$ entries in $[\mathbf{G}^0]$ with the complementary $[\bar{\mathbf{h}}]$ entries in $[\tilde{\mathbf{G}}]$ to obtain $[\mathbf{G}^c]$ as

$$[\mathbf{G}^c] = [\mathbf{G}^o(h) \quad \tilde{\mathbf{G}}(\bar{h})], \tag{18}$$

where $[\tilde{\mathbf{G}}(\bar{h})]$ represents the $[\bar{\mathbf{h}}]$ entries in $[\tilde{\mathbf{G}}]$

If $[\mathbf{G}^c]$ as computed in equation (18) is not truly statically complete (which can be the case because the entries from $[\mathbf{G}^o(h)]$ are not necessarily consistent with the assumed connectivity present in $[\tilde{\mathbf{G}}(\bar{h})]$) the entire procedure can be iterated using $[\mathbf{G}^c]$ as a starting point. The numerical convergence attributes of such an iteration are not addressed in this paper.

4. NUMERICAL RESULTS

4.1. EXAMPLE 1: 2-DOF CANTILEVERED BEAM WITH SINGLE INPUT

Consider the 2-DOF cantilevered beam shown in Figure 2 with parameters

$$EI = 607 \text{ Nm}^2, \qquad \rho A = 1{\cdot}75 \text{ kg/m}, \qquad L = 1{\cdot}5 \text{ m} \tag{19}$$

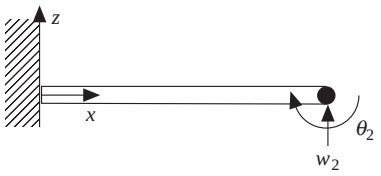

Figure. 2. 2-DOF cantilevered beam model.

and a single input at w_2 so that the DOF sets are

$$\{\mathbf{q}\} = \begin{bmatrix} w_2 \\ \theta_2 \end{bmatrix}, \qquad \{\mathbf{q}_d\} = \{w_2\}, \qquad \{\mathbf{q}_s\} = \{\theta_2\}. \tag{20}$$

Assuming that one mode of the beam is measured, the analytical flexibility matrix $[\mathbf{G}^a]$, the modal flexibility $[\mathbf{G}_n]$, defined as

$$[\mathbf{G}_n] = [\mathbf{\Phi}_n][\mathbf{\Lambda}_n]^{-1}[\mathbf{\Phi}_n], \tag{21}$$

and the dynamically measured flexibility $[\mathbf{G}^0]$ are (as shown in reference [9])

$$[\mathbf{G}^a] = \begin{bmatrix} 1{\cdot}85 & -1{\cdot}85 \\ -1{\cdot}85 & 2{\cdot}47 \end{bmatrix} \times 10^{-3}, \qquad [\mathbf{G}_n] = \begin{bmatrix} 1{\cdot}80 & -1{\cdot}65 \\ -1{\cdot}65 & 1{\cdot}51 \end{bmatrix} \times 10^{-3},$$

$$[\mathbf{G}^o] = \begin{bmatrix} 1{\cdot}85 & -1{\cdot}85 \\ -1{\cdot}85 & 2{\cdot}27 \end{bmatrix} \times 10^{-3}. \tag{22}$$

It should be noted that $[\mathbf{G}_n]$ is not equal to $[\mathbf{G}^a]$ in this case because only the first mode was measured. Theoretically, as more and more modes are measured, the residual flexibility will converge to zero, and both $[\mathbf{G}_n]$ and $[\mathbf{G}^o]$ will converge to $[\mathbf{G}^a]$. The modal flexibility matrix would equal the analytical flexibility matrix in the limit that all modes of the system were measured (because the residual flexibility would go to zero), or in the case that driving point responses were obtained at both degrees of freedom (because the residual flexibility would be fully characterized).

The beams is modelled as a single-element Bernoulli–Euler bending beam (see reference [11] for details). The cross-sectional stiffness parameter EI is assigned an arbitrary initial value of

$$\{EI\} = 1. \tag{24}$$

So the initial statically complete stiffness matrix is

$$[\mathbf{K}] = \begin{bmatrix} 3{\cdot}5556 & 2{\cdot}6667 \\ 2{\cdot}6667 & 2{\cdot}6667 \end{bmatrix}, \tag{25}$$

which is pseudoinverted to get the initial flexibility matrix

$$[\mathbf{G}] = \begin{bmatrix} 1{\cdot}1250 & -1{\cdot}1250 \\ -1{\cdot}1250 & 1{\cdot}5 \end{bmatrix}, \tag{26}$$

which is statically complete, but has not been scaled to approximate $[\mathbf{G}^0(h)]$. The singular value decomposition of $[G]$ yields

$$[\mathbf{V}] = \begin{bmatrix} 0{\cdot}6464 & -0{\cdot}7630 \\ -0{\cdot}7630 & -0{\cdot}6464 \end{bmatrix}, \quad [\mathbf{\Sigma}] = \begin{bmatrix} 2{\cdot}4530 & 0 \\ 0 & 0{\cdot}1720 \end{bmatrix}. \tag{27}$$

Since the input is in the first DOF, the first column in the flexibility matrix is selected as the $[\mathbf{h}]$ set, so that

$$[\mathbf{h}] = \begin{bmatrix} 1 & 1 \\ 2 & 1 \end{bmatrix} \tag{28}$$

and thus

$$[\bar{\mathbf{h}}] = [2 \quad 2]. \tag{29}$$

To select $[\hat{\mathbf{\Sigma}}]$ such that $[\hat{\mathbf{G}}(h)]$ approximates $[G^0(h)]$, form $[\mathbf{C}]$ and $\{\mathbf{B}\}$ as in equation (13) to get

$$[\mathbf{C}] = \begin{bmatrix} 0{\cdot}4178 & 0{\cdot}5822 \\ -0{\cdot}4932 & 0{\cdot}4932 \end{bmatrix}, \qquad \{\mathbf{B}\} = \begin{Bmatrix} 1{\cdot}85 \\ -1{\cdot}85 \end{Bmatrix} \times 10^{-3}; \tag{30}$$

then solve the system of equation (12) to get

$$\{\hat{\mathbf{\Sigma}}\} = \begin{Bmatrix} 0{\cdot}0040 \\ 0{\cdot}0003 \end{Bmatrix}. \tag{31}$$

Selecting $n_c = 2$, the full-rank scaled singular values are determined by solving equation (15) to get

$$\alpha = 0{\cdot}0016. \tag{32}$$

Then $\{\tilde{\mathbf{\Sigma}}\}$ is formed using equation (16) to get

$$\{\tilde{\mathbf{\Sigma}}\} = \begin{Bmatrix} 0{\cdot}0040 \\ 0{\cdot}0003 \end{Bmatrix}. \tag{33}$$

In this case, since n_c was chosen to be the full number of singular values, then $\{\tilde{\mathbf{\Sigma}}\} = \{\hat{\mathbf{\Sigma}}\}$. The synthesized flexibility matrix is formed using equation (17) to get, in m/N units,

$$[\tilde{\mathbf{G}}] = \begin{bmatrix} 1{\cdot}85 & -1{\cdot}85 \\ -1{\cdot}85 & 2{\cdot}47 \end{bmatrix} \times 10^{-3}. \tag{34}$$

Using the $[\mathbf{h}]$ entries of $[\mathbf{G}^a]$ and the $[\bar{\mathbf{h}}]$ entries of $[\tilde{\mathbf{G}}]$ yields the statically complete solution, according to equation (18),

$$[\mathbf{G}^c] = \begin{bmatrix} 1{\cdot}85 & -1{\cdot}85 \\ -1{\cdot}85 & 2{\cdot}47 \end{bmatrix} \times 10^{-3}, \tag{35}$$

which is equal to $[\mathbf{G}^a]$ from equation (21). Thus, for a single element beam, with one continuous measured mode and modal excitation at one DOF, the statically complete flexibility matrix can be determined *exactly* using an arbitrary initial parameter value. As

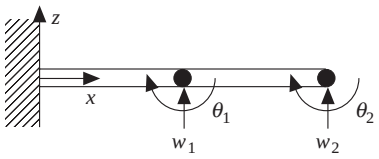

Figure. 3. 4-DOF cantilevered beam model.

shown in reference [9], this compares to 25% error for the modal flexibility $[\mathbf{G}_n]$ and 5% error for the dynamically measured flexibility $[\mathbf{G}^o]$.

4.2. EXAMPLE 2: 4-DOF CANTILEVERED BEAM

Now consider the 4-DOF, 2 element cantilevered beam shown in Figure 3, with the properties listed in equation (19). For this analysis, the elemental model form consists of two Bernoulli–Euler beam elements, and the initial stiffness parameters EI are selected such that they are equal. There is once again a single input at w_2 so that the DOF sets are

$$\{\mathbf{q}\} = \begin{Bmatrix} w_1 \\ \theta_1 \\ w_2 \\ \theta_2 \end{Bmatrix}, \qquad \{\mathbf{q}_d\} = \{w_2\}, \qquad \{\mathbf{q}_s\} = \begin{Bmatrix} w_1 \\ \theta_1 \\ \theta_2 \end{Bmatrix}. \tag{36}$$

The entries in the third column of the dynamically measured flexibility $[\mathbf{G}^o]$ are selected as the $[\mathbf{h}]$ entries, because the input is at the third DOF. The convergence of the percent error in the 2-Norm of the flexibility matrix, $\|\Delta G\|/\|G\|$, as the number of measured modes increases, for the three different measures of flexibility, is shown in Figure 4. This measure of error indicates that the statically complete flexibility $[\mathbf{G}^c]$ has zero error for any number of measured modes. In this case, the method once again obtains the exact solution for the statically complete flexibility.

In order to further demonstrate the ability of the full-rank flexibility estimation algorithm to correctly identify the flexibility matrix, consider the same 2-element, 4-DOF beam structure, but now let the EI value of the tip element equal 90% of its nominal value.

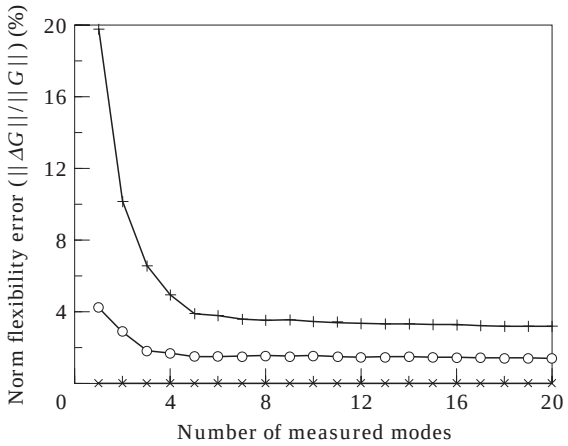

Figure 4. Convergence of norm G error for 2-element cantilevered beam; +, $[\mathbf{G}_n]$; ○, $[\mathbf{G}^o]$; ×, $[\mathbf{G}^c]$.

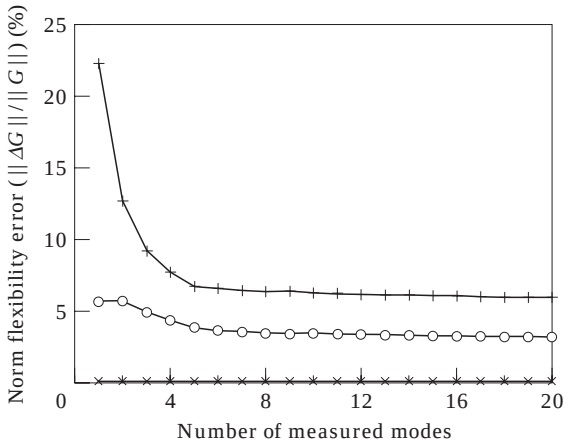

Figure 5. Convergence of norm G error for 2-element cantilevered beam with reduced stiffness 1 element: key as in Figure 4.

This could represent, for example, a loss of load-carrying capability due to structural cracking.

For this case, the flexibility norm error convergence is shown in Figure 5. Comparing these results to the results for the two-element uniform beam shown in Figure 4, it is clear that the overall error level is higher for the modal and rank-deficient residual flexibility solutions, but still nearly zero for the full-rank solution. Thus, the full-rank solution is able to iteratively determine the actual element stiffnesses, even when the initial values of the stiffnesses are assumed to be equal. It takes about 20 iterations for the full-rank solution to converge in this case.

This two-element example with non-uniform stiffness is important because it demonstrates the validity of the proposed method for a more complicated situation than that of a uniform beam. For instance, the uniform two-element or one-element problems could be solved by using the first modal frequency to compute the stiffness coefficient EI. This coefficient could then be used to scale the elemental stiffness matrix in equation (25), and then determine the global analytical stiffness and flexibility matrices directly. For the non-uniform beam example, such an approach will not work dependably because the combination of elemental stiffnesses that will produce a given set of frequencies is not necessarily unique. The use of the proposed technique to determine the flexibility matrix converges as shown, however, because both measured mode shapes and measured modal frequencies are used.

5. EXPERIMENTAL RESULTS

A series of modal vibration tests was performed on a simple cantilevered beam structure to study the computation of a statically complete flexibility matrix from a dynamically measured flexibility matrix. The test setup for this structure is shown in the photo of Figure 6. A schematic of the test structure is shown in Figure 7, including the instrumentation and test input location. The test parameters and modal parameter identification procedure used are described in reference [9]. The identified frequencies, modal damping ratios, and mode shape descriptions for the cantilevered beam structure are listed in Table 1. Two analyses were performed on the data: one using a single-element, 2-DOF discretization, as shown in Figure 2, and one using a two-element, 4-DOF discretization, as shown in Figure 3.

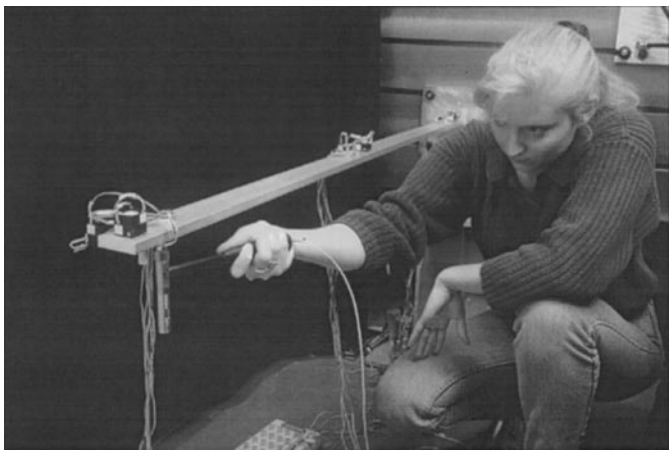

Figure 6. Cantilevered beam test setup.

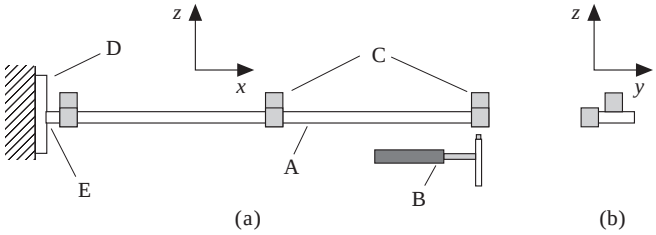

Figure 7. Schematic of cantilevered beam test structure: A, aluminium beam; B, modal impact hammer; C, triaxial accelerometers; D, aluminium base plate; E, welded connection. (a) Side view, (b) end view.

For the single-element discretization, the global DOF set is defined as in equation (20). The measured mass-normalized mode shapes of the first four modes with respect to the global DOF are

$$[\boldsymbol{\Phi}] = \begin{bmatrix} -1{\cdot}0609 & -0{\cdot}9915 & 0{\cdot}8500 & 0{\cdot}6313 \\ 3{\cdot}5428 & 4{\cdot}0249 & -5{\cdot}2349 & -3{\cdot}4299 \end{bmatrix} \tag{37}$$

and the measured modal frequencies in Hz are

$$\{\boldsymbol{\omega}\} = \begin{Bmatrix} 4{\cdot}34 \\ 27{\cdot}06 \\ 77{\cdot}55 \\ 149{\cdot}47 \end{Bmatrix}. \tag{38}$$

TABLE 1

Identified modal frequencies and damping ratios for cantilevered beam experiment

Frequency (Hz)	Damping Ratio (%)	Mode description
4·34	0·058	First bending
27·06	0·508	Second bending
77·55	0·309	Third bending
149·47	0·378	Fourth bending

The measured partition of the residual flexibility, also converted to global DOF, is

$$[\mathbf{G}_r] = \begin{bmatrix} 0{\cdot}0004 & -0{\cdot}0184 \\ -0{\cdot}0184 & 0{\cdot}5561 \end{bmatrix} \times 10^{-3}, \tag{39}$$

where rank $([\mathbf{G}_r]) = 1$ because there is only one modal excitation DOF. The modal flexibility is formed by substituting the quantities of equations (37) and (38) into equation (21) to get

$$[\mathbf{G}_n] = \begin{bmatrix} 0{\cdot}0016 & -0{\cdot}0052 \\ -0{\cdot}0052 & 0{\cdot}0176 \end{bmatrix}. \tag{40}$$

The residual can be included to obtain the dynamically measured flexibility

$$[\mathbf{G}^o] = \begin{bmatrix} 0{\cdot}0016 & -0{\cdot}0052 \\ -0{\cdot}0052 & 0{\cdot}0181 \end{bmatrix}. \tag{41}$$

Since the input was applied vertically near the tip, the correlation set is chosen to be the vertical tip displacement with respect to a vertical tip input. This corresponds to the (1, 1) entry of $[\mathbf{G}^o]$. So, using $[\mathbf{G}^o]$ as the starting point and $[\mathbf{h}] = [1 \;\; 1]$, the statically complete flexibility estimation method is applied to get

$$[\mathbf{G}^c] = \begin{bmatrix} 0{\cdot}0016 & -0{\cdot}0019 \\ -0{\cdot}0019 & 0{\cdot}0023 \end{bmatrix}. \tag{42}$$

The accuracy of the statically complete flexibility matrix can be assessed by comparing it to the analytical flexibility matrix

$$[\mathbf{G}^a] = \begin{bmatrix} 0{\cdot}0018 & -0{\cdot}0018 \\ -0{\cdot}0018 & 0{\cdot}0024 \end{bmatrix}. \tag{43}$$

The flexibility matrix solutions are compared in Table 2. It is evident that the statically complete flexibility matrix $[\mathbf{G}^c]$ is much more accurate with respect to the analytical solutions than the modal or dynamically measured flexibility matrices. It should be noted, however, that the fact that the experimental boundary most likely does not represent a perfect cantilever may also account for some of the difference between $[\mathbf{G}^c]$ and $[\mathbf{G}^a]$. A more valid measure of accuracy would be to compare $[\mathbf{G}^c]$ to a set of directly measured static displacements.

For the two-element discretization, the modal flexibility and the dynamically measured flexibility are both computed as in the single-element analysis, except that the DOF sets are defined as in equation (36). The statically complete solution is also computed, but now

TABLE 2

Percentage norm error in flexibility matrices for the cantilevered beam experiment

Model discretization	$[\mathbf{G}_n]$	$[\mathbf{G}^o]$	$[\mathbf{G}^c]$
1-Element model	406	418	7·0
2-Element model	434	448	9·6

the correlation global displacements are selected to be $\{w_2\}$ and $\{w_1\}$, with respect to input at $\{w_2\}$. This means that the correlation entries in **[G]** are (3, 3) and (1, 3). It should be noted that (3, 1) could also be included in the correlation set, but because of the symmetric parameterization of the statically complete flexibility, this constraint is redundant. The results of this 2-element analysis are shown in Table 2. As with the 1-element results, the large errors in the estimated global rotations create large errors in the modal and dynamically measured flexibility matrices. However, the statically complete flexibility matrix is not constrained to fit the measured rotations, and therefore produces much more accurate results.

CONCLUSION

The dynamically measured flexibility matrix has been proven in previous research to be a valuable tool for structural modelling and damage diagnosis using modal data. The primary limitation of the dynamically measured flexibility matrix is its inability to reproduce the correct static force-displacement behavior between all of the measured DOF due to the limited number of modes which are measured. The method presented in this paper provides a means for overcoming the limitations of dynamically measured flexibility by scaling an analytical, statically complete flexibility matrix such that it approximates the statically complete coefficients from the dynamically measured flexibility matrix. The method can be implemented using only linear solution techniques, and requires the assumption of a set of finite elements and elemental connectivity. Both numerical and experimental results have been presented to demonstrate the validity of the technique for improving the accuracy of the measured flexibility matrix.

ACKNOWLEDGMENTS

This paper reports work supported by Sandia National Laboratories under Contract No. AJ-4223 with Dr. George H. James III and Dr. John R. Red-Horse as technical monitors. Also, the authors wish to recognize University of Colorado undergraduate students Ms. Nikki Robinson and Ms. Trudy Schwartz for their contributions to the experimental portion of this research. Support for the first author was also provided by Los Alamos National Laboratory Directed Research and Development Project #95002. This work was performed under the auspices of the United States Department of Energy.

REFERENCES

1. A. E. Aktan, K. L. Lee, C. Chuntavan and T. Aksel 1994 *Proceedings of* 12*th International Modal Analysis Conference*, Honolulu, HI, 462–468. Modal testing for structural identification and condition assessment of constructed facilities.
2. T. Toksoy and A. E. Aktan 1994 *Experimental Mechanics* **34**, 271–278. Bridge-condition assessment by modal flexibility.
3. N. A. Robinson, L. D. Peterson, G. H. James and S. W. Doebling 1996 *Proceedings of* 14*th International Modal Analysis Conference*, Dearborn, MI, 857–865. Damage detection in aircraft structures in using dynamically measured static flexibility matrices.
4. A. K. Pandey and M. Biswas 1995 *Modal Analysis*: *The International Journal of Analytical and Experimental Modal Analysis* **10**, 104–117. Damage diagnosis of truss structures by estimation of flexibility change.
5. S. W. Doebling, C. R. Farrar, M. B. Prime and D. W. Shevitz 1996 *Los Alamos National Laboratory report LA*13070-*MS*. Damage identification and health monitoring of structural and mechanical systems from changes in their vibration characteristics: a literature review.

6. D. R. Martinez, T. G. Carne, D. L. Gregory and A. K. Miller 1984 *Proceedings of 25th AIAA/ASME Structures, Structural Dynamics, and Materials Conference*, AIAA Paper 84–0941. Combined experimental/analytical modelling using component mode synthesis.
7. J. R. Admire, M. L. Tinker and E. W. Ivey 1994 *AIAA Journal* **32**, 170–175. Residual flexibility test method for verification of constrained structural models.
8. J. D. Hinkle, L. D. Peterson and S. W. Doebling 1996 *Journal of Spacecraft and Rockets* **33**, 848–852. Analysis of nonlinear mechanisms in a precision deployable structure using measured flexibility.
9. S. W. Doebling, L. D. Peterson and K. F. Alvin 1996 *AIAA Journal* **34**, 1678–1685. Estimation of reciprocal residual flexibility from experimental modal data.
10. G. Strang 1988 *Linear Algebra and its Applications*. San Diego: Harcourt Brace Jovanovich.
11. T. Y. Yang 1986 *Finite Element Structural Analysis*. Englewood Cliffs, NJ: Prentice-Hall.

NOMENCLATURE

$\{\mathbf{F}\}$	applied static load vector
$[\mathbf{G}]$	static flexibility matrix
$[\mathbf{G}^a]$	analytically predicted static flexibility matrix
$[\mathbf{G}^c]$	statically complete flexibility matrix approximated using dynamically measured flexibility
$[\mathbf{G}^o]$	dynamically measured flexibility matrix (including residual flexibility)
$[\mathbf{G}_r]$	residual flexibility matrix
$[h]$, $[\bar{h}]$	indices of entries in dynamically measured flexibility matrix which are statically complete, and the complementary set of indices
$[\mathbf{K}]$	global structural stiffness matrix
$\{\mathbf{u}\}$	static displacement vector
$[\mathbf{V}]$	matrix of flexibility matrix singular vectors
$[\mathbf{\Phi}_n]$	measured vibration mode shape matrix
$[\mathbf{\Lambda}_n]$	diagonal matrix of measured structural eigenvalues
$[\mathbf{\Sigma}]$	diagonal matrix of flexibility matrix singular values
$\{\boldsymbol{\omega}\}$	vector of measured modal frequencies